Progress In Electromagnetics Research Letters, Vol. 69, 87–92, 2017

A Compact Polarization Diversity UWB MIMO Antenna with a Fork-Shaped Decoupling Structure

Hui-Fen Huang* **and Shu-Guang Xiao**

Abstract—A compact polarization diversity ultra-wideband (UWB) antenna with size $32 \times 32\,\mathrm{mm}^2$ is presented in this paper. The proposed antenna consists of a linear tapered slot **(LTS)** ground, two orthogonal micro-strip feed lines and a floating fork-shaped decoupling structure located diagonally across the two orthogonal microstrip feed lines. The ground is in one side of the substrate, and the feed lines and the decoupling structure are in the other side. In addition, two rectangular slots are made in both the ground and feed lines to widen impedance bandwidth. Simulated and measured results indicate that the band covers from 3.1 to 12 GHz with $S_{11} < -10\,\mathrm{dB}$ and $S_{12} < -15\,\mathrm{dB}$.

1. INTRODUCTION

Ultrawideband (UWB) [1] technology has many promising features in the modern wireless portable communication devices, for example, wide bandwidths, low power consumption, high-speed communication transmission rate, good radiation pattern performance, and steady impedance. However, UWB systems also bear channel fading in the multipath environment, similar to a lot of other wireless communication systems. As a solution to this problem without using extra transmitted power or frequency spectrum in rich scattering environments, antennas incorporated with diversity technology have been presented [2, 3].

Various UWB diversity antennas have been previously reported. For instance, the antenna elements are arranged orthogonally to obtain polarization diversity and high isolation [4–11]. In order to enhance wideband isolation, a protruded stub integrated diagonally in the ground plane was used in [6–8, 11]; a rectangular slot in the circular radiator was used in [6]; a parasitic T-shaped strip between the radiating elements was used in [9]. However, some decoupling structures are complex.

In this letter, a compact polarization diversity UWB with simple fork-shaped decoupling structure located diagonally across the two orthogonal microstrip feed lines. In addition, two rectangular slots are made in both the ground and feed lines to widen impedance bandwidth. The paper is organized as follows. Section 2 provides the antenna design and analysis. Section 3 shows the measured results. The conclusion is given in Section 4.

2. ANTENNA DESIGN

2.1. Antenna Description

Figure 1 shows a diagrammatic sketch of the proposed polarization diversity UWB antenna consisting of a LTS ground, two orthogonal micro-strip feed lines and a floating fork-shaped decoupling structure (circled by green triangle). The prototype is shown in Fig. 2. The decoupling structure is

Received 19 June 2017, Accepted 12 July 2017, Scheduled 22 July 2017

* Corresponding author: Hui-Fen Huang (huanghf@scut.edu.cn).

The authors are with the School of Electronic and Information Engineering, South China University of Technology, Guangzhou, China.

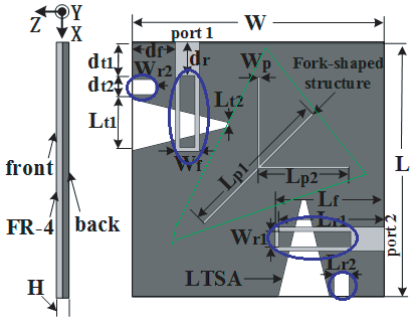

Figure 1. Geometry of the proposed antenna.

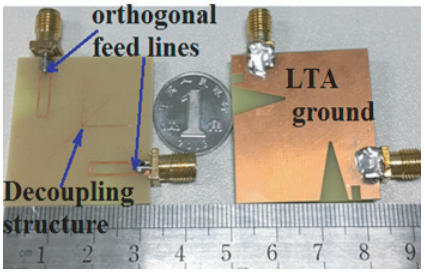

Figure 2. Prototype of the proposed antenna.

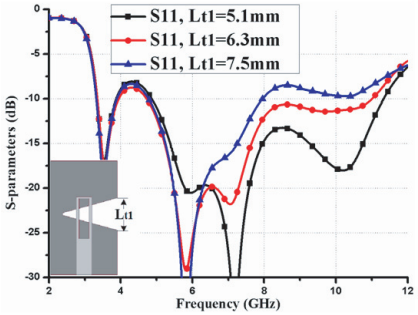

Figure 3. S_{11} with different L_{t1}.

located diagonally across the two orthogonal microstrip feed lines. The antenna is made on an FR4 substrate (thickness 1.6 mm, relative permittivity 4.4 and loss tangent 0.02). The ground is in one side of the substrate, and the feed lines and the decoupling structure are in the other side. Two rectangular slots (marked in blue circles in Fig. 1) are cut both in the ground and two feed lines to widen impedance bandwidth. Optimized parameters are (units: mm): $H = 1.6$, $L = W = 32$, $L_{t1} = 6.6$, $L_{t2} = 0.6$, $L_{r1} = 13.4$, $L_{r2} = 2$, $L_f = 13.8$, $L_{p1} = 19.6$, $L_{p2} = 11.5$, $d_{t1} = 4.4$, $d_{t2} = 2.5$, $W_{r1} = 2$, $W_{r2} = 3$, $W_f = 3$, $d_f = 5.5$, $d_r = 4.2$, $W_p = 0.2$. These final values of the antenna dimensions were obtained by parameter optimization using the commercial software Ansoft HFSS [12]. All constituents and geometry parameters are marked in Fig. 1 and Fig. 2.

2.2. Impedance Bandwidth Analysis

Figure 3 shows the S_{11} with three different LTS open angles L_{t1} in the ground. The bandwidth increases with the decrease of the opening angle of the tapered slot. Hence, the opening angles of LTS in the ground obviously influence impedance width. Steps for further improving the impedance width by rectangular slots are described in Fig. 4 (named from Antenna-1 to Antenna-3), and the corresponding S_{11} curves are in Fig. 5. The rectangular slots greatly improve the -10 dB impedance bandwidth, finally covering the whole UWB 3.1–10.6 GHz.

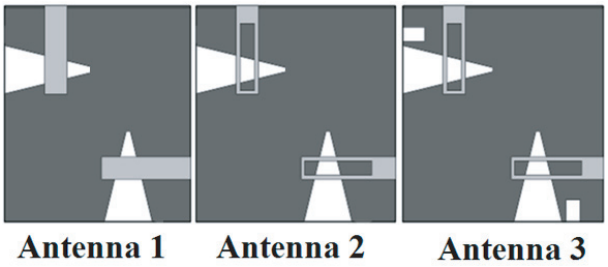

Figure 4. Steps for further improving impedance width by rectangular slots.

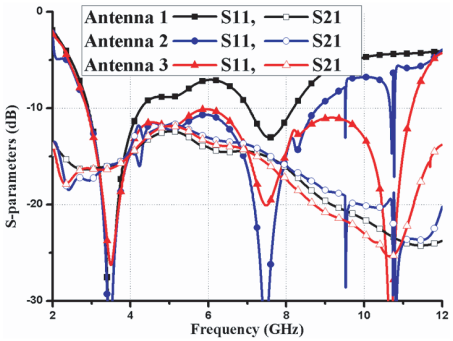

Figure 5. S_{11} for Antenna 1–3.

2.3. Decoupling Analysis

2.3.1. Geometery Parameter Effect on Decoupling

Figure 6 shows the decoupling structure evolution from decoupling line (marked Antenna 4) to fork-shaped structure (Antenna 5). The isolation and return loss for Antennas 4, 5 are shown in Fig. 7. The

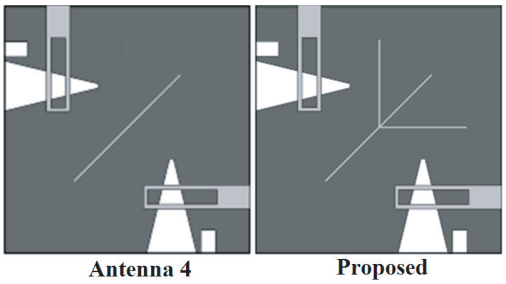

Figure 6. Decoupling structure evolution.

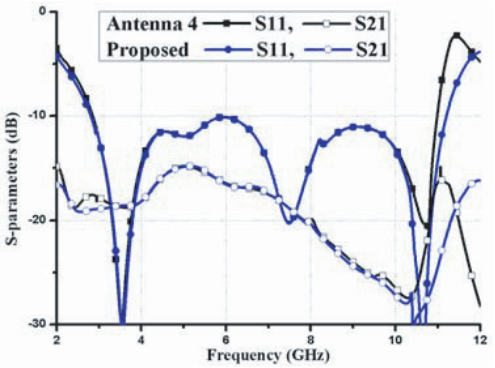

Figure 7. S parameters for Fig. 6.

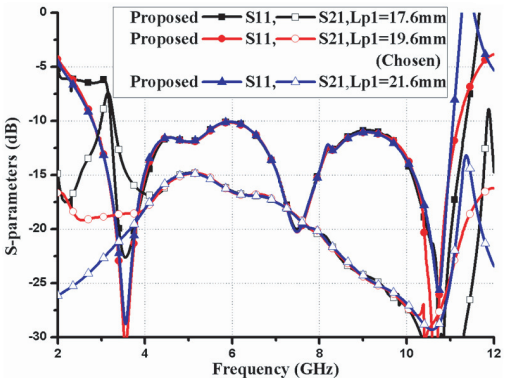

Figure 8. S-parameters with different width L_{p1}.

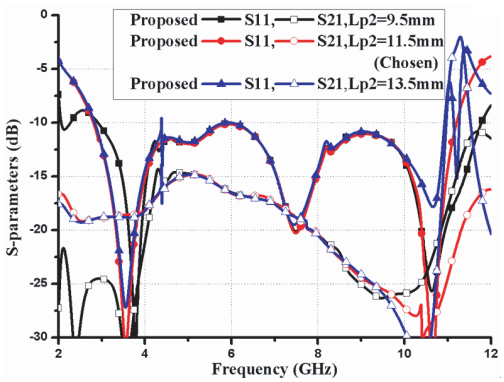

Figure 9. S-parameters with different width L_{p2}.

decoupling line can basically solve coupling problem, and the fork-shaped decoupling structure further improves impedance width and isolation in the high band above 10 GHz. The effects of parameters L_{p1} and L_{p2} on decoupling are shown in Fig. 8 and Fig. 9. Longer L_{p1} contributes to the isolation for the lower band, but does in the opposite direction for the higher band. Compared with L_{p1} in decoupling, parameter L_{p2} is in the other way around.

From the bandgap of view, the fork-shaped structure on the middle ground makes the resonant frequency of the antenna fall inside the bandgap of the fork-shaped structure. Surface waves are suppressed, and the mutual coupling is reduced then. From the electrical length of view, apparently, the different actual physical lengths of each branch leads to different electrical lengths. The different electrical lengths directly correspond to different frequencies to decouple. In other words, different branches work at different frequencies to reduce the coupling between two antenna elements.

2.3.2. Surface Current Analysis

Figures 10(a), (b) are the surface current distributions for antennas with/without decoupling fork-shaped structure, on the condition that port 1 is excited while port 2 is terminated to a matching load. Compared with Fig. 10(a), the current from port 1 to port 2 is dramatically reduced.

3. MEASURED RESULT

The simulated and measured results are shown in Fig. 11. $S_{11} < -10$ dB and $S_{12} < -15$ dB in the whole UWB 3.1–10.6 GHz. Fig. 12 indicates that gain is 1.5 dBi–4.1 dBi, and efficiency is above 70% in the UWB band. In Fig. 13, derived from the measured 3D E-field radiation patterns [13], the envelope

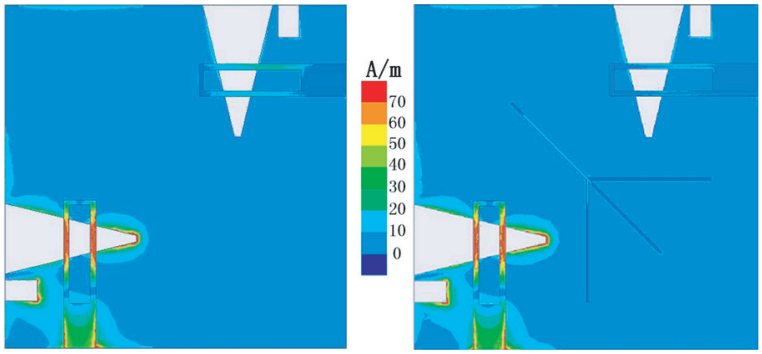

Figure 10. Surface current distribution at 7 GHz.

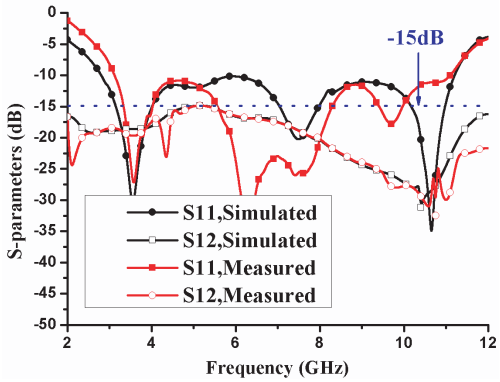

Figure 11. Simulated and measured *S*-parameters.

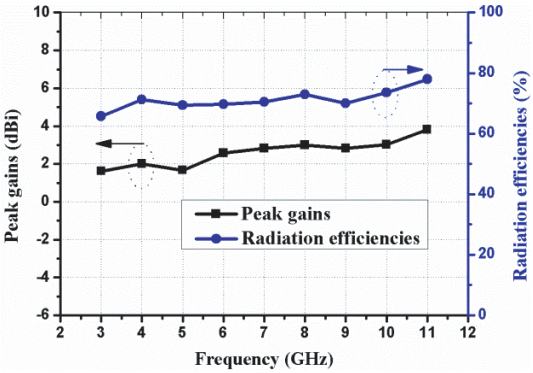

Figure 12. Measured gains and radiation efficiencies.

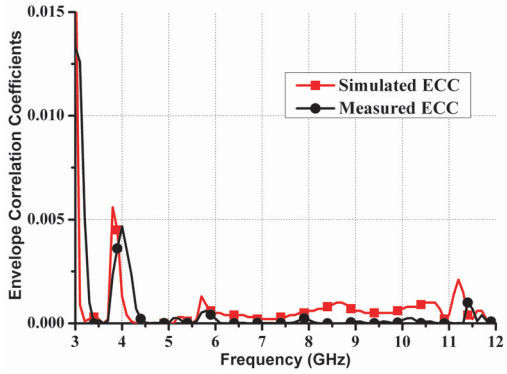

Figure 13. Simulated and measured *ECC*.

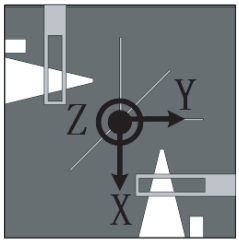

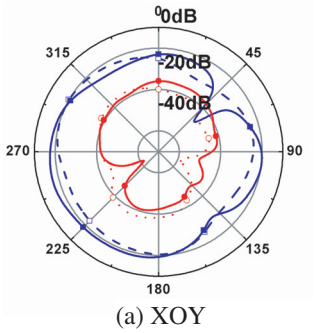

(a) XOY

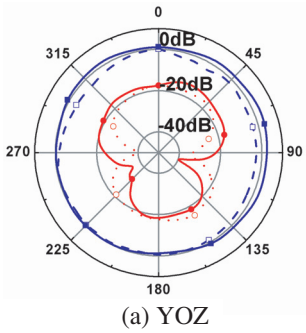

(a) YOZ

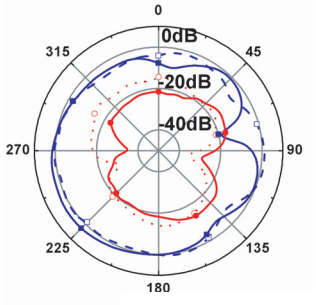

(b) XOY

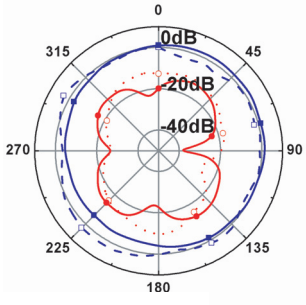

(b) YOZ

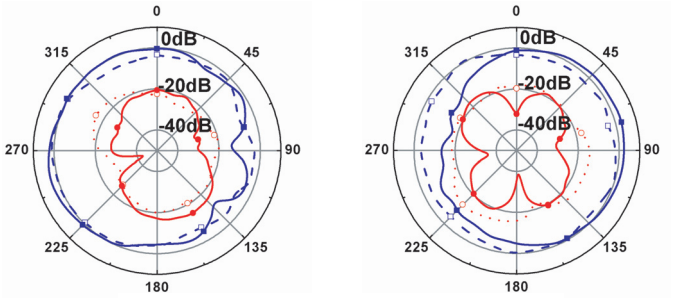

(c) XOY (c) YOZ

Figure 14. Radiation patterns of the XOY, YOZ plane: at (a) 4.5 GHz; (b) 7.5 GHz; (c) 9.5 GHz.

correlation coefficient (ECC) is below 0.02, ensuring good diversity performance. Table 1 shows a comparison of this antenna with some other UWB polarization diversity works. In Fig. 14, the H-plane pattern is nearly omnidirectional [14]. Low cross-polarisation can also be seen in Fig. 14. The S-parameters are measured by the Agilent R3770 vector network analyzer, and a Satimo chamber [15] is used to measure the radiation patterns, realized gains and efficiency. The discrepancy between the simulated and measured results may be due to the SMA connector and environment of measurement.

Table 1. Comparison with the recent compact UWB polarization diversity antennas.

Reference	[4]	[5]	[6]	[7]	[8]	[9]	[10]	[11]	**This**
Dimension (mm^2)	60×30	35×35	41×41	50×50	48×48	38.5×38.5	65×65	48×48	$\mathbf{32 \times 32}$
Min. Isolation (dB)	20	14	14	15	15	15	40	15	**15**
$f_L - f_H$ (GHz)	2.8–11	3–12	3–12	2.76–10.75	2.5–12	3.08–11.8	2.75–11	2.35–11	**3.1–10.7**

4. CONCLUSION

In this paper, a compact polarization diversity UWB MIMO antenna with size $32 \times 32\,mm^2$ is developed. A simple fork-shaped decoupling structure located diagonally across the two orthogonal microstrip feed lines contributes to the high isolation between two ports. $S_{12} < -15$ dB, $S_{11} < -10$ dB, $ECC < 0.02$ in the whole UWB 3.1–10.6 GHz.

ACKNOWLEDGMENT

This work is supported by the National Natural Science Foundation of China under Grant 61071056, Natural Science Foundation of Guangdong Province under Grant 2016A030313462 and Education of Guangdong Province Characteristic innovation Foundation under Grant 2014KTSCX017.

REFERENCES

1. Lim, E. G., Z. Wang, C. U. Lei, Y. Wang, and K. Man, "Ultra wideband antennas — Past and present," *Iaeng International Journal of Computer Science*, Vol. 37, No. 3, 304–314, 2010.
2. Zhao, N. and W.-P. Tian, "CPW-fed dual-band MIMO antenna with common radiating element," *Progress In Electromagnetics Research Letters*, Vol. 62, 71–75, 2016.
3. Kaiser, T., F. Zheng, and E. Dimitrov, "An overview of ultra-wide-band systems with MIMO," *Proc. IEEE*, Vol. 97, No. 2, 285–312, 2009.

4. Huang, H., Y. Liu, S. S. Zhang, and S. X. Gong, "Compact polarization diversity ultrawideband MIMO antenna with triple band-notched characteristics," *Microwave Opt. Technol. Lett.*, Vol. 57, 946–953, 2015.
5. Zhu, J. F., S. F. Li, B. T. Feng, L. Deng, and S. X. Yin, "Compact dual-polarized UWB quasi-self-complementary MIMO/diversity antenna with band-rejection capability," *IEEE Antennas Wireless Propag. Lett.*, Vol. 15, 905–908, 2016.
6. Srivastava, G. and B. K. Kanuijia, "Compact dual band-notched UWB MIMO antenna with shared radiator," *Microwave Opt. Technol. Lett.*, Vol. 57, 2886–2891, 2015.
7. Chacko, B. P., G. Augustin, and T. A. Denidni, "Uniplanar polarisation diversity antenna for ultrawideband systems," *IET Microw. Antennas Propag.*, Vol. 7, No. 10, 851–857, 2013.
8. Gao, P., S. He, X. B. Wei, Z. Q. Xu, N. Wang, and Y. Zheng, "Compact printed UWB diversity slot antenna with 5.5-GHz band-notched characteristics," *IEEE Antennas Wireless Propag. Lett.*, Vol. 13, 376–379, 2014.
9. Kang, L., H. Li, X. H. Wang, et al., "Compact offset microstrip-fed MIMO antenna for band-notched UWB applications," *IEEE Antennas Wireless Propag. Lett.*, Vol. 14, 1754–1757, 2015.
10. Huang, H., Y. Liu, and S. X. Gong, "Uniplanar differentially driven UWB polarisation diversity antenna with bandnotched characteristics," *Electronics Letters*, Vol. 51, No. 3, 206–207, 2015.
11. Huang, H., Y. Liu, S. S. Zhang, and S. X. Gong, "Uniplanar ultrawideband polarization diversity antenna with dual band-notched characteristics," *IEEE Antennas Wireless Propag. Lett.*, Vol. 13, 1745–1748, 2014.
12. http://www.ansoft.com/products/hf/hfss/.
13. Vaughan, R. G. and J. B. Andersen, "Antenna diversity in mobile communication," *IEEE Trans. Veh. Technol.*, Vol. 36, No. 4, 149–172, 1987.
14. Wong, K. L., *Planar Antennas for Wireless Communications*, Wiley-IEEE Press, 2003.
15. Satimo, [online] Available: http://www.satimo.com/.